ISSN 2664-4169 (Print) & ISSN 2664-7923 (Online)
South Asian Research Journal of Biology and Applied Biosciences
Abbreviated Key Title: South Asian Res J Bio Appl Biosci

| Volume-8 | Issue-5 | Sep-Oct -2026 | **DOI: https://doi.org/10.36346/sarjbab.2026.v08i05.005**

Original Research Article

In vitro Cytotoxicity and *In silico* Screening Evaluation of *Clitoria ternatea* L. Flower Methanolic Extract against Cancer Cell Lines

Sukaina Abbas[1]*, Tejashree V. Shanbhag[1]

[1]Department of Life Sciences, Kishinchand Chellaram College, HSNC University, Mumbai, Vidyasagar Principal K.M. Kundnani Chowk, 124, Dinshaw Vacha Rd, Churchgate, Mumbai, Maharashtra 400-020

***Corresponding Author:** Sukaina Abbas
Department of Life Sciences, Kishinchand Chellaram College, HSNC University, Mumbai, Vidyasagar Principal K.M. Kundnani Chowk, 124, Dinshaw Vacha Rd, Churchgate, Mumbai, Maharashtra 400-020

Article History
Received: 28.07.2026
Accepted: 22.09.2026
Published: 26.10.2026

Abstract: *Clitoria ternatea* L. (Fabaceae) flowers are used widely in traditional medicine and are rich in anthocyanins. The methanolic extract of this flower was screened for phytochemical classes, profiled by GC-MS, and tested by MTT assay against HeLa, MCF-7, and A549 cells. Ten GC-MS-identified compounds were carried forward for ADMET prediction (ADMETlab 3.0) and molecular docking (AutoDock Vina) against six targets: EGFR (1M17), estrogen receptor α (3ERT), MDM2 (4HFZ), a Bcl-2/Bcl-xL chimera (2W3L), tubulin at the colchicine site (1SA0), and KRAS G12S (7TLG). Protein–ligand interactions were profiled with PLIP. The extract reduced viability in a concentration-dependent manner in all three lines, with IC50 values of 66.94 µg/mL (HeLa), 146.48 µg/mL (MCF-7), and 372.32 µg/mL (A549). HeLa cells were the most sensitive and A549 was the least sensitive cell line. Palmitic acid had the strongest support of evidence: published caspase-3-mediated cytotoxicity, the lowest predicted mutagenicity of the ten compounds, and salt-bridge interactions at two of the six targets. DDMP built the most specific hydrogen-bond network, at EGFR, though its predicted mutagenicity and carcinogenicity were both elevated. Overall, the extract shows cell-line-dependent cytotoxicity.

Keywords: ADMET, *Clitoria ternatea*, GC-MS, Molecular Docking, MTT Assay, Cytotoxicity Assay, PLIP, Cervical Cancer, Breast Cancer, Lung Cancer.

INTRODUCTION

Clitoria ternatea L. (Fabaceae), commonly called butterfly pea, is a leguminous vine cultivated across tropical Asia for ornamental and medicinal use. It is used traditionally as a nootropic, anxiolytic, antipyretic, and anti-inflammatory agent. Phytochemical studies of *C. ternatea* report flavonoids, anthocyanins, terpenoids, and fatty-acid derivatives across different plant parts and solvents.

Several *C. ternatea* preparations have demonstrated cytotoxic or antiproliferative activity. Cytotoxicity has been reported in a brine-shrimp-lethality study (Islam *et al.,* 2023). Ethanolic flower extracts have shown activity against MCF-7 cells (Rahayu *et al*., 2023); and against HEp-2 cells (Shen *et al*., 2016). A methanol/water extraction study reported moderate cytotoxicity against several cancer cell lines, including MCF-7, MDA-MB-231, and Caov-3 (Neda *et al*., 2013). Cyclotides isolated from *C. ternatea*, produced a two- to four-fold reduction in the IC50 of paclitaxel in a paclitaxel-resistant A549 sub-line, indicating chemosensitization (Zhang *et al*., 2013). A methanolic leaf extract has separately been reported to reduce HL60 leukaemia cell viability in a dose-dependent manner (Das *et al*., 2020), and a methanolic flower extract has been reported to induce apoptosis in MCF-7 cells, with an IC50 of 27.2 µg/mL with increased caspase-3 activity (Shivaprakash *et al*., 2015).

Despite these findings, the relationship between the chemical composition of C. ternatea flower extracts and their specific anticancer targets remains insufficiently characterized. GC-MS screening provides the chemical fingerprint of

Copyright © 2026 The Author(s): This is an open-access article distributed under the terms of the Creative Commons Attribution **4.0 International License (CC BY-NC 4.0)** which permits unrestricted use, distribution, and reproduction in any medium for non-commercial use provided the original author and source are credited.

these extracts. This can be narrowed down by ranking them on predicted affinity for a target linked to the disease. ADMET prediction filters out compounds likely to fail on absorption or toxicity grounds. The present study integrates phytochemical screening, GC-MS profiling, ADMET prediction and molecular docking to investigate the potential of *C. ternatea* flowers. Cytotoxicity was assessed against HeLa, MCF-7, and A549 cancer cell lines for an in vitro assessment. This workflow links the extract's cytotoxicity to its potential chemical constituents and molecular targets.

MATERIALS AND METHODS

Plant Material and Extract Preparation

Fresh flowers of *Clitoria ternatea* L. were collected, shade-dried at room temperature, and powdered. The powder was extracted with methanol by Soxhlet extraction; the extract was filtered, concentrated to dryness, and stored at 4 °C in an airtight container. The dried extract was used for phytochemical screening, GC-MS analysis, and all subsequent work.

Qualitative Phytochemical Screening

The extract was screened for thirteen phytochemical classes using standard qualitative colour and precipitation tests: alkaloids (ammoniacal chloroform extraction, dilute sulphuric acid), saponins (ether-hydrochloric acid precipitation), flavonoids (Shinoda test), tannins and phenols (ferric chloride test), steroids and terpenoids (Liebermann–Burchard reaction), cardiac glycosides (Keller-Kiliani test), gums and mucilage (aqueous-alcohol precipitation), fatty acids (filter-paper spot test), proteins/amino acids (ninhydrin test), carbohydrates (Benedict's test), and anthocyanins (dilute hydrochloric acid test) (Shaikh and Patil, 2020).

GC-MS Analysis

GC-MS analysis was carried out through Aaranya Biosciences Pvt. Ltd., Chennai, on a Shimadzu GCMS-QP2020 fitted with a fused-silica capillary column (30 m × 0.25 mm i.d. × 0.25 µm film thickness). Helium (99.99%) was the carrier gas at 1 mL/min. A 1 µL sample was injected in split mode (1:10) at an injector temperature of 230 °C, with a solvent cut time of 3–5 min. The oven program started at 40 °C (held 3 min), ramped at 7 °C/min to 180 °C (held 1 min), then ramped at 25 °C/min to 250 °C (held 13.20 min), for a total run time of 40 min. Ion-source and interface temperatures were 230 °C and 250 °C; mass spectra were acquired over 30–450 m/z. Compounds were identified against the NIST 14 library, and the retention time, area percentage, and similarity index (SI) of the top hit were recorded for every peak in the integrated chromatogram. Each compound was checked against its NIST spectra, and structures used for docking were built from the reported name and formula. One peak (20.815 min, 40.94% of total area, SI 84) matched tris(hydroxymethyl)nitromethane, an industrial nitroalcohol with no reported occurrence in Fabaceae. Since this is chemically implausible as a genuine floral constituent, it was excluded from ADMET and docking and is reported here only for completeness of the chromatographic record. The remaining ten peaks, 59.06% of total area, were carried forward and are reported with their SI scores (Table 3).

In Vitro Cytotoxicity Assay (MTT)

HeLa, MCF-7, and A549 cells were obtained from Sasaam Biologicals, Chennai, and maintained in Minimal Essential Medium (MEM; HiMedia) with 10% fetal bovine serum (FBS; Cistron), penicillin (100 U/mL), and streptomycin (100 µg/mL) at 37 °C in 5% CO_2. Cytotoxicity was assessed by the MTT assay of Mosmann (1983). Cells (1×10^5/well) were seeded in 24-well plates and grown to confluence; the extract was then added at eight concentrations (1000, 500, 250, 125, 62.5, 31.2, 15.6, and 7.8 µg/mL) alongside an untreated control, and plates were incubated for 24 h. Wells were washed with serum-free MEM/PBS (pH 7.4), and 100 µL of 0.5% MTT (5 mg/mL) was added and incubated for 4 h. Formazan was solubilized in 1 mL DMSO per well and read at 570 nm against a DMSO blank. Percentage viability was (A570 treated / A570 control) × 100. Each concentration was tested in triplicate wells. Dose–response data for each line were fitted to a variable-slope logistic model (Top constrained to 100% and Bottom to 0%) to obtain IC50 values with 95% confidence intervals.

Target Selection and Receptor Preparation

Six crystal structures were selected from the RCSB Protein Data Bank to match the biology of the three cell lines and general cytotoxicity mechanisms: the EGFR kinase domain (1M17), the estrogen receptor α ligand-binding domain (3ERT), the MDM2 N-terminal domain (4HFZ), KRAS carrying the G12S mutation reported for A549 (7TLG; Tate *et al*., 2019), a Bcl-2/Bcl-xL chimera (2W3L), and tubulin at the colchicine site (1SA0). For each target, a single chain (or the minimal biologically relevant chain set) was extracted and water and crystallization additives were removed. Structures were protonated at pH 7.4 with PDB2PQR 3.7.1 using PROPKA and the AMBER force field (Dolinsky *et al.*, 2007), then converted to rigid PDBQT format in Open Babel (O'Boyle *et al.,* 2011) with Gasteiger charges. Docking box centers and dimensions for each target, defined from the native ligand's coordinates (or, for MDM2, the p53-peptide contact residues Phe19/Trp23/Leu26) plus 4–6 Å padding, are given in Table 1.

Table 1: The six protein targets used for docking, with PDB identifiers and the AutoDock Vina grid-box center and dimensions defined for each

PDB ID	Target	Grid center (Å): x, y, z	Grid size (Å): x × y × z
1M17	EGFR kinase domain	21.697, 0.303, 52.093	23.71 × 12.68 × 15.10
3ERT	ERα ligand-binding domain	30.282, -1.913, 24.206	20.45 × 16.76 × 20.69
4HFZ	MDM2 N-terminal domain	-1.226, -16.732, 7.652	25.10 × 21.66 × 17.50
2W3L	Bcl-2/Bcl-xL chimera	38.905, 26.949, -12.545	18.58 × 19.57 × 18.35
1SA0	Tubulin, colchicine site	118.921, 89.718, 5.931	18.52 × 20.23 × 16.09
7TLG	KRAS G12S, switch-II pocket	5.894, -21.093, -8.339	21.05 × 14.78 × 19.30

ADMET and Druglikeness Prediction

ADMET properties of the ten compounds identified by GC-MS were predicted with ADMETlab 3.0 (https://admetlab3.scbdd.com), a DMPNN-based platform covering 119 endpoints (Fu *et al*., 2024). Batch SMILES were submitted, and hERG channel-blocking probability, drug-induced liver injury (DILI), Ames mutagenicity, carcinogenicity, A549 cytotoxicity probability, and QED are reported (Table 4).

Molecular Docking

Three-dimensional structures of the ten compounds were built from SMILES in RDKit (Landrum, n.d.; ETKDG embedding, MMFF94 minimization) and converted to flexible PDBQT format with Meeko. Docking was performed in AutoDock Vina 1.2.5 (Trott & Olson, 2010; Eberhardt *et al*., 2021) at an exhaustiveness of 8, nine poses per ligand, against each target box from the previous section. The top-ranked pose for each compound–target pair was kept for interaction analysis.

Protein–Ligand Interaction Analysis

The top-ranked pose of each compound at each target was merged with the corresponding protonated receptor to form a complex, and interactions were profiled with PLIP 3.0.1 (Schake *et al*., 2025), which reports hydrogen bonds, hydrophobic contacts, salt bridges, π-stacking, π-cation interactions, halogen bonds, and water bridges using default geometric cutoffs.

Statistical Analysis

IC50 values and 95% confidence intervals (profile likelihood) were obtained by non-linear regression of a four-parameter logistic model (variable slope, Bottom constrained to 0 and Top constrained to 100) against mean percentage viability at each concentration (n = 3 wells per concentration) in GraphPad Prism 10.6, with fit quality reported as R^2.

RESULTS

Qualitative Phytochemical Screening

The phytochemical screening results are discussed in Table 2, with the diagnostic test used for each class. Terpenoid, cardiac-glycoside, fatty-acid, carbohydrate, and anthocyanin responses were positive; flavonoids were weakly positive; alkaloids, saponins, tannins, steroids, phenols, gums/mucilage, and proteins/amino acids were not detected.

Table 2: Qualitative phytochemical screening of the *C. ternatea* flower methanolic extract. Positive: terpenoids, cardiac glycosides, fatty acids, carbohydrates, anthocyanins (strong response, consistent with the flower origin of the extract). Weak positive: flavonoids. Absent: alkaloids, saponins, tannins, steroids, phenols, gums/mucilage, proteins/amino acids

Assay	Test	Result
Alkaloids	Ammoniacal chloroform extraction test	Absent
Saponin	Ether-HCl precipitation test	Absent
Flavonoids	Shinoda test	Weak positive (+/-)
Tannins	Ferric chloride test	Absent
Steroids	Liebermann-Burchard test	Absent
Terpenoids	Liebermann-Burchard test	Positive
Cardiac glycosides	Keller-Kiliani test	Positive
Phenol	Ferric chloride test	Absent
Gums and mucilage	Aqueous-alcohol precipitation test	Absent
Fatty acids	Filter-paper spot test	Positive
Protein / amino acid	Ninhydrin test	Absent
Carbohydrate	Benedict's test	Positive
Anthocyanin	Dilute HCl test	Positive

GC-MS Profiling and Compound Identification Confidence

The GC-MS spectrum confirmed the presence of multiple components eluting at different retention times. The mass spectrometer analyses each eluted compound to determine its structure from its fragmentation pattern: as a compound breaks apart under electron ionization, the resulting fragments appear as peaks at characteristic mass-to-charge (m/z) ratios, and this fragmentation pattern acts as a fingerprint that can be matched against a reference library. Identification here was based on the NIST 14 library. Eleven peaks were resolved, accounting for the full integrated chromatogram (100.00% of total area; Table 3). The peak at 20.815 min (40.94% of total area, SI 84) matched tris(hydroxymethyl)nitromethane, an industrial nitroalcohol with no reported occurrence in Fabaceae, and was excluded from ADMET and docking; the remaining ten peaks (59.06% of total area) were carried forward. The methyl-glucohexodialdo-furanoside (20.51%) and glyceraldehyde (12.02%) were the largest peaks among the retained compounds; diethylene glycol monostearate (0.27%) was the smallest. SI scores across the retained compounds ranged from 60 (hexadecadienol) to 86 (palmitic acid).

Table 3: GC-MS-identified compounds in the *C. ternatea* flower methanolic extract (NIST 14 library match), with retention time, peak area, molecular formula, and similarity index (SI). *Peak 6 (tris(hydroxymethyl)nitromethane) was excluded from ADMET and docking

Peak	RT (min)	Area %	Compound	Formula	MW	SI
1	8.340	3.45	Dihydroxyacetone	C3H6O3	90	75
2	13.805	1.93	2,3-dihydro-3,5-dihydroxy-6-methyl-4H-pyran-4-one (DDMP)	C6H8O4	144	73
3	14.846	12.02	Glyceraldehyde	C3H6O3	90	82
4	16.255	4.26	Glyceryl monoacetate	C5H10O4	134	79
5	17.389	5.90	Methoxy-trimethyl-1,3-dioxolane	C7H14O3	146	72
6*	20.815	40.94	Tris(hydroxymethyl)nitromethane	C4H9NO5	151	84
7	24.592	6.45	β-D-Arabinopyranose	C5H10O5	150	78
8	25.143	20.51	Methyl-glucohexodialdo-furanoside	C7H12O6	192	82
9	27.191	3.16	Palmitic acid	C16H32O2	256	86
10	28.631	1.11	Hexadecadienol	C16H30O	238	60
11	28.800	0.27	Diethylene glycol monostearate	C22H44O4	372	66

In Vitro Cytotoxicity

The extract reduced viability in a concentration-dependent manner in all three lines across 7.8–1000 µg/mL (Figure 1). Four-parameter logistic regression gave IC50 values of 66.94 µg/mL (95% CI 24.15–185.56, $R^2 = 0.978$) for HeLa, 146.48 µg/mL (95% CI 109.03–196.78, $R^2 = 0.998$) for MCF-7, and 372.32 µg/mL (95% CI 222.48–623.08, $R^2 = 0.997$) for A549. HeLa cells were the most sensitive and A549 the least.

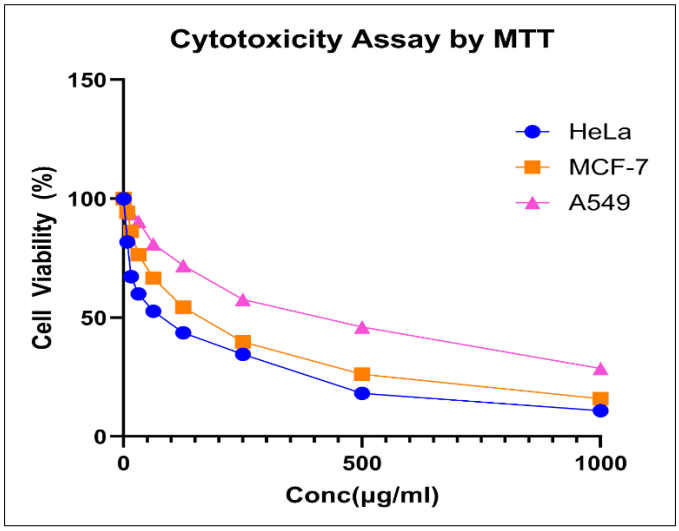


Figure 1. Cytotoxicity of the *C. ternatea* flower methanolic extract (CTFE) against A549, HeLa, and MCF-7 cells, expressed as % cell viability vs. concentration (µg/mL). Curves and IC50 values were fitted from triplicate wells at each concentration.

HeLa cell morphology after 24 h treatment is shown in Figure 2, MCF-7 in Figure 3, and A549 in Figure 4; rounding, shrinkage, and reduced monolayer density increased with concentration in all three lines, most pronounced at 1000 µg/mL.

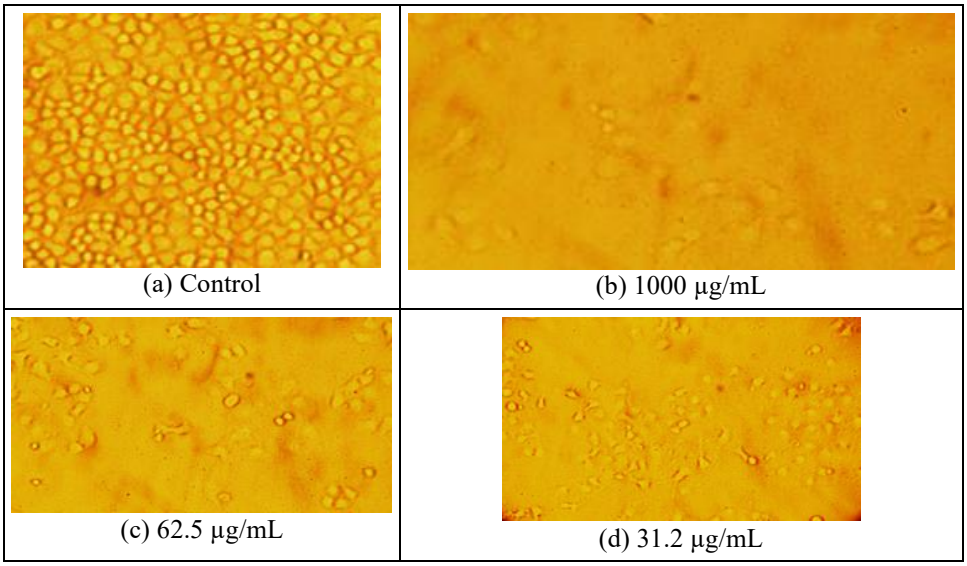


Figure 2: HeLa cell morphology after 24 h treatment with the extract, MTT assay: (a) control, (b) 1000 µg/mL, (c) 62.5 µg/mL, (d) 31.2 µg/mL.

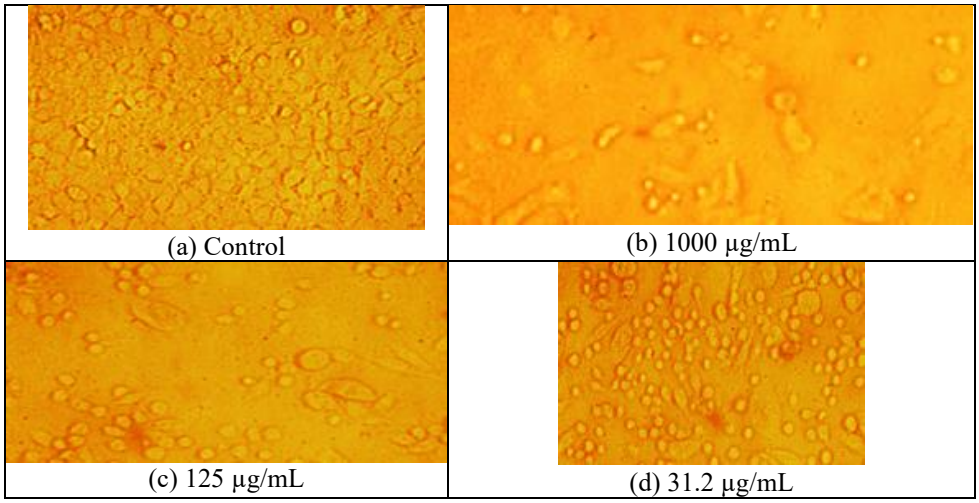


Figure 3: MCF-7 cell morphology after 24 h treatment with the extract, MTT assay: (a) control, (b) 1000 µg/mL, (c) 125 µg/mL, (d) 31.2 µg/mL.

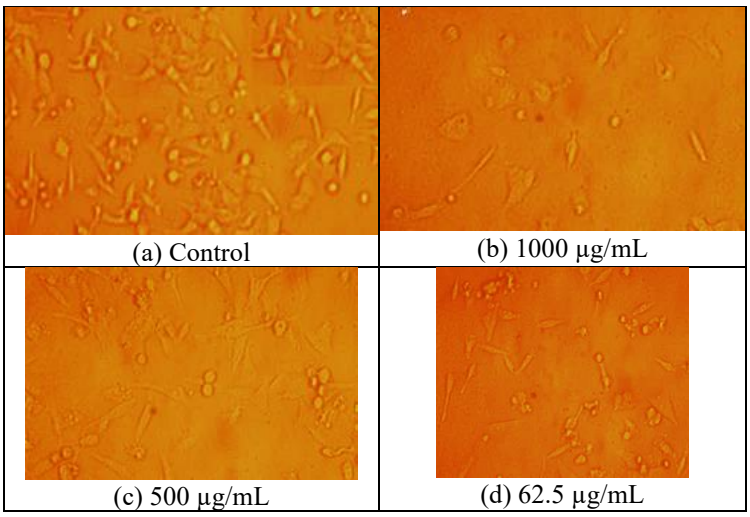


Figure 4: A549 cell morphology after 24 h treatment with the extract, MTT assay: (a) control, (b) 1000 µg/mL, (c) 500 µg/mL, (d) 62.5 µg/mL.

ADMET and Druglikeness Screening

ADMET profiles vary widely across the panel (Table 4). DDMP carries the highest predicted mutagenicity and carcinogenicity, followed by the methyl-glucohexodialdo-furanoside (mutagenicity) and the methoxy-trimethyl-dioxolane (carcinogenicity); palmitic acid and diethylene glycol monostearate have the lowest mutagenicity. Hexadecadienol has the highest predicted A549 cytotoxicity in the panel, and diethylene glycol monostearate the highest hERG liability; the small polyols and sugars score low on both toxicity and predicted cytotoxicity.

Table 4: ADMETlab 3.0-predicted endpoints (probability, 0–1; bins: <0.1 excellent, 0.1–0.3 good, 0.3–0.5 medium, 0.5–0.7 medium-high, 0.7–0.9 high, >0.9 very high). DDMP has a mid-range QED score (0.491) with the highest predicted AMES mutagenicity (0.823) and carcinogenicity (0.879). Hexadecadienol has the highest predicted A549 cytotoxicity (0.535); palmitic acid the lowest AMES score (0.047); diethylene glycol monostearate the highest hERG liability (0.819)

Compound	hERG	DILI	AMES	Carcino-genicity	A549 cytotox.	QED
Dihydroxyacetone	0.142	0.044	0.409	0.581	0.002	0.435
DDMP	0.089	0.690	0.823	0.879	0.011	0.491
Glyceraldehyde	0.239	0.043	0.342	0.231	0.021	0.407
Glyceryl monoacetate	0.178	0.026	0.723	0.297	0.022	0.481
Methoxy-trimethyl-dioxolane	0.556	0.596	0.678	0.851	0.015	0.555
β-D-Arabinopyranose	0.483	0.145	0.605	0.229	0.024	0.304
Methyl-glucohexodialdo-furanoside	0.355	0.595	0.796	0.360	0.040	0.519
Palmitic acid	0.439	0.188	0.047	0.270	0.112	0.413
Hexadecadienol	0.607	0.020	0.253	0.083	0.535	0.374
Diethylene glycol monostearate	0.819	0.112	0.105	0.527	0.150	0.204

Molecular Docking

Docking affinities for all ten compounds against all six targets are shown in Figure 6. Hexadecadienol had the highest mean affinity (−5.55 kcal/mol) and ranked in the top three at every target. Palmitic acid ranked in the top three at five targets. The methyl-glucohexodialdo-furanoside bound most strongly to KRAS G12S (−6.34 kcal/mol). Dihydroxyacetone and glyceraldehyde ranked lowest at every target.

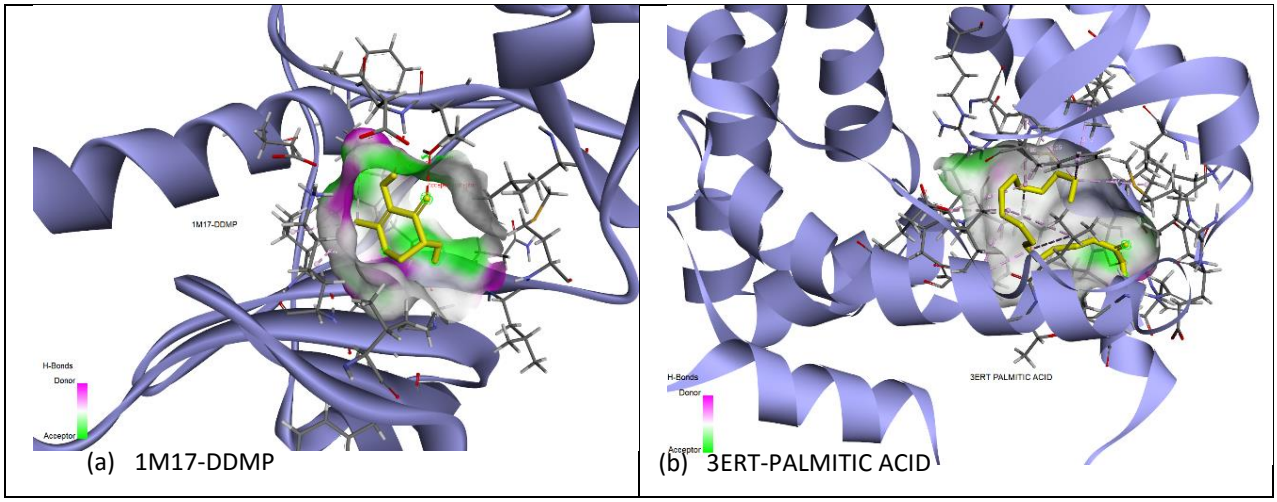


Figure 5: Three-dimensional docking: (A) DDMP at the EGFR kinase domain (1M17), forming five hydrogen bonds within the ATP-binding pocket. (B) Palmitic acid at the estrogen receptor α ligand-binding domain (3ERT), including the salt-bridge interaction with His524. Receptor shown as ribbon; ligand (yellow) and interacting residues shown as sticks; binding-pocket surface coloured by hydrogen-bond donor (magenta) to acceptor (green) gradient.

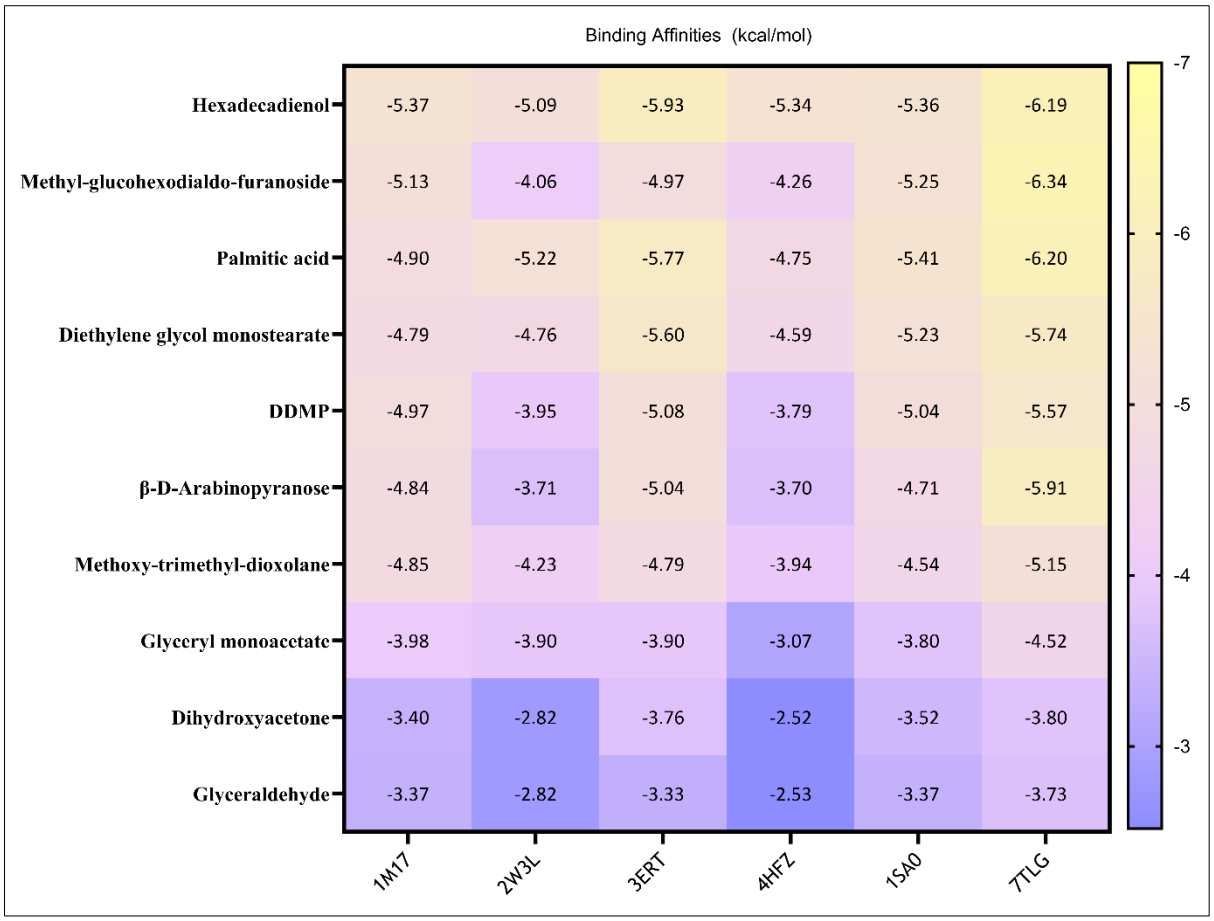


Figure 6: Binding affinities (kcal/mol) for the compounds against all six targets. 1M17-EGFR kinase domain, 2W3L-Bcl-2/Bcl-xL, 3ERT-ERα ligand-binding domain, 4HFZ-MDM2 N-terminal domain, 1SA0-Tubulin, 7TLG-KRAS

Protein–Ligand Interaction Analysis (PLIP)

Table 5 gives the interacting residues and bond counts for each compound-target pair. DDMP and the small sugars (dihydroxyacetone, glyceraldehyde, β-D-arabinopyranose) are polar-dominated, with many hydrogen bonds and little or no hydrophobic contact; hexadecadienol, palmitic acid, and diethylene glycol monostearate are hydrophobic-dominated. Salt bridges are rare overall and occur mainly in palmitic acid, diethylene glycol monostearate, β-D-arabinopyranose, and the furanoside.

Table 5: PLIP-derived interacting residues and non-covalent bond counts (HB = hydrogen bond, HP = hydrophobic contact, SB = salt bridge) for each compound at each target. DDMP forms five hydrogen bonds at EGFR (Glu738, Thr766, Gln767, Thr830, Asp831), more than any other compound at that target, and no salt bridges anywhere. Palmitic acid forms salt bridges at two targets (ERα, His524; KRAS G12S), as does diethylene glycol monostearate (Bcl-2/Bcl-xL; KRAS G12S). The furanoside forms the most salt bridges overall (five across the panel, three at the KRAS switch-II pocket). — indicates no interaction detected in any of PLIP's categories for that pose, not a missing measurement

Compound	1M17	2W3L	3ERT	4HFZ	1SA0	7TLG
DDMP	LEU764, THR766, GLU738, GLN767, THR830, ASP831 *2HP / 5HB*	PHE63, PHE71, ALA108 *2HP / 1HB*	ALA350, LEU387, ARG394, PHE404 *2HP / 4HB*	LEU57, ILE61, PHE91, ILE99 *4HP*	PRO175, GLN176, SER178, THR353 *9HB*	VAL9, ILE100, GLU63, ARG68, ASP69, ARG102 *2HP / 5HB*
Palmitic acid	LEU694, VAL702, ALA719, LYS721, LEU768,	PHE63, TYR67, ASP70, PHE71, VAL92,	LEU346, ALA350, LEU384, LEU387, LEU391,	LEU54, LEU57, ILE61, PHE91,	ALA180, LEU248, LYS254, LEU255, ASN258,	VAL9, GLU62, TYR64, ARG68, TYR96,

Compound	1M17	2W3L	3ERT	4HFZ	1SA0	7TLG
	MET769, LEU820, GLU738, THR766, ASP831 *8HP / 4HB*	LEU96, ALA108, PHE112, GLU95 *13HP / 2HB*	PHE404, LEU428, LEU525, GLU419, GLY420, HIS524 *10HP / 3HB / 1SB*	VAL93, GLN72 *7HP / 1HB*	LYS352, ALA317 *7HP / 2HB*	GLN99, ILE100, VAL103, LYS16 *10HP / 2SB*
Hexadecadienol	LEU694, VAL702, ALA719, LYS721, MET769, LEU820, THR766 *9HP / 3HB*	PHE63, TYR67, ASP70, PHE71, VAL92, LEU96, ALA108, PHE112 *12HP*	LEU346, ALA350, LEU384, PHE404, ILE424, LEU525, LEU387, ARG394 *9HP / 4HB*	LEU57, ILE61, TYR67, PHE91, VAL93, ILE99, TYR100 *9HP / 2HB*	LEU248, ALA250, LEU255, ASN258, ALA316, LYS352, ALA317, ALA354 *8HP / 5HB*	VAL9, GLU62, TYR64, ARG68, MET72, TYR96, GLN99, ILE100, VAL103, GLY10, LYS16 *12HP / 3HB*
Diethylene glycol monostearate	LEU694, VAL702, ALA719, LEU820, LYS721, GLU738, GLN767, MET769 *4HP / 4HB*	PHE63, TYR67, ASP70, PHE71, LEU96, PHE112, GLY104, ARG105 *9HP / 3HB / 1SB*	LEU346, LEU349, ALA350, LEU384, LEU387, LEU391, PHE404, ILE424, LEU525 *13HP*	LEU57, ILE61, TYR67, PHE91, VAL93, ILE99, TYR100, GLN72 *8HP / 2HB*	LEU248, LYS254, LEU255, ASN258, ALA316, LYS352, ALA354, ASN101 *10HP / 3HB*	VAL9, GLU62, TYR64, MET72, TYR96, ILE100, VAL103, GLY10, SER12, ASP92, LYS16 *9HP / 4HB / 1SB*
Dihydroxyacetone	LYS721, THR766 *3HB*	ARG98, ASP99, ARG105 *4HB*	GLU353, LEU387, ARG394, PHE404 *6HB*	LEU54 *1HB*	PRO175, GLN176, SER178, THR353 *8HB*	GLY10, SER12, LYS16, THR58, TYR96 *6HB*
Glyceraldehyde	LYS721, THR766 *4HB*	GLU95, LEU96, ASP99 *3HB*	LEU387, ARG394, PHE404 *6HB*	—	PRO175, GLN176, SER178, VAL351, THR353 *9HB*	GLY10, LYS16, THR58, ALA59, ARG68, TYR96 *7HB*
Glyceryl monoacetate	LEU820, ALA719, LYS721, GLU738, THR766 *1HP / 4HB*	ASP70, PHE71, ALA108 *2HP / 2HB*	LEU384, LEU346, GLU353, LEU387, ARG394 *1HP / 4HB*	LEU54, ILE99 *2HP*	GLN11, ALA12, GLY142, GLU183 *2HP / 2HB*	GLU62, LYS16, THR58, ALA59, GLN61, GLU63, ARG68 *1HP / 7HB / 1SB*
Methoxy-trimethyl-dioxolane	LYS721, LEU764, LEU820 *3HP*	PHE63, TYR67, PHE71, PHE112	LEU346, ALA350, LEU387, PHE404	LEU54, LEU57, PHE91, ILE99	LEU248, LYS254, LYS352 *3HP*	TYR64, GLN99, ILE100,

Compound	1M17	2W3L	3ERT	4HFZ	1SA0	7TLG
		4HP	*4HP*	*4HP*		VAL103, ARG68 *5HP / 2HB*
β-D-Arabinopyranose	LYS721, GLU738, ASP831 *4HB / 1SB*	ALA108 *1HB*	ALA350, GLU353, LEU387, ARG394, PHE404 *5HB / 1SB*	GLN72 *2HB*	PRO175, SER178, LYS352, THR353 *8HB*	GLY10, SER12, THR58, GLN61, ARG68, TYR96, LYS16 *10HB / 1SB*
Methyl-glucohexodialdo-furanoside	LYS721, GLU738, THR766, GLN767, ASP831 *1HP / 4HB / 1SB*	LEU96, ALA108, PHE112 *2HP / 2HB*	GLU353, LEU387, PHE404, ARG394 *3HB / 1SB*	VAL93, GLY58, MET62, GLN72 *1HP / 4HB*	LYS352, ASN349, THR353 *1HP / 4HB*	GLN61, GLU63, LYS16, ARG68 *2HB / 3SB*

DISCUSSION

Clitoria ternatea has a long history of use in traditional medicine, where it has been applied as a nootropic, anxiolytic, antipyretic, and anti-inflammatory agent. Its flowers are a known source of anthocyanins, and recent work has looked at the plant's anticancer potential more closely, tying specific activity to cyclotides, anthocyanins, and phenolic compounds. The present results add to that record by testing one extract across three matched cell lines and linking the result to specific molecular targets.

The extract reduced viability in all three lines in a dose-dependent way, with a sensitivity order (HeLa > MCF-7 > A549). The MCF-7 IC50 found here, 146.48 µg/mL, is lower than the 175.35 µg/mL reported for a methanol/water extract (Neda et al., 2013), but higher than the 27.2 µg/mL reported for a methanolic extract that used caspase-3 activation as evidence of apoptosis (Shivaprakash *et al*., 2015). Palmitic acid from *Musa paradisiaca* induces caspase-3-mediated apoptosis in human oral squamous cell carcinoma (Budi *et al*., 2022), and palmitic acid from a marine alga causes cell-cycle arrest and cytotoxicity in leukemic cells. In this study it has the lowest predicted mutagenicity of the ten compounds and forms salt bridges at two targets (His524 at ERα; a Lys16/Arg68 cluster at KRAS G12S). DDMP forms the most specific hydrogen-bond network in the study, five bonds at EGFR, matching how EGFR-flavonoid studies explain inhibitory activity (Dipa *et al*., 2025). DDMP has been previously documented for its antioxidant activity and in vivo protective effects against oxidative organ damage. However, to the best of our knowledge, its potential anticancer activity and interactions with the six targets investigated in the present study have not been previously reported. While ADMET predictions indicate potential mutagenic and carcinogenic liabilities that were not captured by QED-based screening, these computational findings warrant further toxicological evaluation. Hexadecadienol ranked in the top three of the ten compounds at every target and showed the highest predicted A549 cytotoxicity in the panel. Its PLIP profile was almost entirely hydrophobic, with no salt bridges at any target, the same pattern used elsewhere to rule out candidate compounds in a Bcl-2 screen (Alkhathami *et al*., 2025). That points to a membrane-level effect rather than binding to one specific protein.

As shown in Figure 6, which ranks all ten compounds by their best-pose Vina binding affinity across the six targets, β-D-arabinopyranose, dihydroxyacetone, and glyceraldehyde form many hydrogen bonds by raw count, yet dihydroxyacetone and glyceraldehyde rank lowest at every target and β-D-arabinopyranose ranks in the lower half at four of the six targets. Small polar molecules with several donor/acceptor groups can form many weak contacts without the shape match required for effective binding. Dihydroxyacetone causes cytotoxic and genotoxic effects in A549 cells through mitochondrial stress and DNA damage (Hernandez *et al*., 2024). Glyceraldehyde is a known protein-cross-linking, ROS-generating mutagen (Usui *et al*., 2004). The small sugars illustrate that hydrogen-bond count alone is a poor proxy for genuine target engagement. More broadly, the fact that palmitic acid, DDMP, and hexadecadienol each stand out on a different axis — safety, specificity, and affinity respectively — suggests the extract's cytotoxicity is unlikely to trace back to one compound and argues for further exploration of the crude extract's multimodal action.

CONCLUSIONS

The methanolic extract of *Clitoria ternatea* L. flowers reduced cell viability in a dose-dependent way across all three lines, with IC50 values of 66.94, 146.48, and 372.32 µg/mL for HeLa, MCF-7, and A549— a HeLa > MCF-7 > A549

order of sensitivity. GC-MS identified ten compounds in the extract. Combining the docking, ADMET, and PLIP results, palmitic acid stands out as the strongest candidate: it has independent literature support, the lowest predicted mutagenicity in the panel, and salt-bridge interactions at two of the six targets. DDMP and hexadecadienol also showed binding and cytotoxicity signals worth following up. The next steps are bioassay-guided isolation of palmitic acid and DDMP, direct testing of these compounds against the three cell lines, and in vivo work to confirm the extract's cytotoxic potential.

Acknowledgements

The authors thank Aaranya Biosciences Pvt. Ltd., Chennai, for GC-MS analysis, and Sasaam Biologicals, Chennai, for procuring the HeLa, MCF-7, and A549 cell lines used in this study.

Authors' Contributions

Sukaina Abbas conceived and designed the study, performed the formal analysis, curated the data, carried out the investigation, and wrote the original draft. Tejashree V. Shanbhag conceived and designed the study, acquired funding, reviewed and edited the manuscript, and supervised and administered the project. Both authors read and approved the final version of the manuscript.

Abbreviations:

ADMET, absorption/distribution/metabolism/excretion/toxicity; AMES, Ames mutagenicity assay; DILI, drug-induced liver injury; GC-MS, gas chromatography–mass spectrometry; hERG, human ether-a-go-go-related gene; IC50, half-maximal inhibitory concentration; MTT, 3-(4,5-dimethylthiazol-2-yl)-2,5-diphenyltetrazolium bromide; PDB, Protein Data Bank; PLIP, Protein–Ligand Interaction Profiler; QED, quantitative estimate of druglikeness; SI, similarity index; SMILES, simplified molecular-input line-entry system.

Competing Interests: The authors declare that there are no competing interests.

Funding: This work was supported by HSNC University, Mumbai (Grant No. HSNCU/RDC/MRP-2/2026/03/March/2026).

REFERENCES

- Alkhathami, A. G., Alshahrani, M. Y., Asiri, M., & Wahab, S. (2025). Phytochemicals Daturilinol and Withametelin B identified as novel Bcl2 inhibitors via virtual screening and molecular simulations. Scientific Reports, 15. https://doi.org/10.1038/s41598-025-99901-0
- Budi, H. S., Anitasari, S., Ulfa, N. M., Setiabudi, M. A., Ramasamy, R., Wu, C. Z., & Shen, Y. K. (2022). Palmitic acid of Musa Paradisiaca induces apoptosis through caspase-3 in human oral squamous cell carcinoma. European Review for Medical and Pharmacological Sciences, 26(19), 7099–7114.
- Das, A., Shanmuga Priya, G., Soundariya, S., Deepesh, P., Edwin, A. R., Vihashinee, E., Rubiga, A., Megavarthini, S., Eswaran, R., & Bindhu, J. (2020). Antibacterial and in vitro anticancer study of methanol extracts of *Clitoria ternatea* leaves. Journal of Natural Remedies, 20(2), 96–102.
- Dipa, C. D., Hossain, S., Chy, M. M. K., Rahman, M. S. F., Kayes, T., Easha, A. M., Moin, A. T., Vakare, S. N., Patil, R. B., & Sarkar, B. K. (2025). In silico exploration of anticancer plant phytochemicals for EGFR-targeted lung cancer therapy. Scientific Reports, 15, 27809.
- Dolinsky, T. J., Czodrowski, P., Li, H., Nielsen, J. E., Jensen, J. H., Klebe, G., & Baker, N. A. (2007). PDB2PQR: expanding and upgrading automated preparation of biomolecular structures for molecular simulations. Nucleic Acids Research, 35(Web Server issue), W522–W525.
- Eberhardt, J., Santos-Martins, D., Tillack, A. F., & Forli, S. (2021). AutoDock Vina 1.2.0: new docking methods, expanded force field, and Python bindings. Journal of Chemical Information and Modeling, 61, 3891–3898.
- Fu, L., Shi, S., Yi, J., Wang, N., He, Y., Wu, Z., et al. (2024). ADMETlab 3.0: an updated comprehensive online ADMET prediction platform enhanced with broader coverage, improved performance, API functionality and decision support. Nucleic Acids Research, 52(W1), W422–W431.
- Hernandez, A., Hedlich-Dwyer, J., Hussain, S., Levi, H., Sonavane, M., Suzuki, T., Kamiya, H., & Gassman, N. R. (2024). Acute exposure to dihydroxyacetone promotes genotoxicity and chromosomal instability in lung, cardiac, and liver cell models. Toxicological Sciences, 201(1), 85–102.
- Islam, M. A., Mondal, S. K., Islam, S., Shorna, M. N. A., Biswas, S., Uddin, M. S., Zaman, S., & Saleh, M. A. (2023). Antioxidant, cytotoxicity, antimicrobial activity, and in silico analysis of the methanolic leaf and flower extracts of *Clitoria ternatea*. Biochemistry Research International, 2023, 8847876.
- Landrum, G. (n.d.). RDKit: open-source cheminformatics software. https://www.rdkit.org
- Mosmann, T. (1983). Rapid colorimetric assay for cellular growth and survival: application to proliferation and cytotoxicity assays. Journal of Immunological Methods, 65, 55–63.

- Neda, G. D., Rabeta, M. S., & Ong, M. T. (2013). Chemical composition and anti-proliferative properties of flowers of *Clitoria ternatea*. International Food Research Journal, 20(3), 1229–1234.
- O'Boyle, N. M., Banck, M., James, C. A., Morley, C., Vandermeersch, T., & Hutchison, G. R. (2011). Open Babel: an open chemical toolbox. Journal of Cheminformatics, 3, 33.
- Rahayu, S., Muhtadi, M., & Indrayudha, P. (2023). Apoptosis induction activity and inhibition of MCF-7 cell proliferation in active isolate of butterfly pea flower (*Clitoria ternatea* L.). Trends in Sciences.
- Schake, P., Bolz, S. N., Linnemann, K., & Schroeder, M. (2025). PLIP 2025: introducing protein-protein interactions to the protein-ligand interaction profiler. Nucleic Acids Research, 53(W1), W463–W465.
- Shaikh, J. R., & Patil, M. (2020). Qualitative tests for preliminary phytochemical screening: an overview. International Journal of Chemical Studies, 8(2), 603–608.
- Shen, Y., Du, L., Zeng, H., Zhang, X., Prinyawiwatkul, W., Alonso-Marenco, J. R., & Xu, Z. (2016). Butterfly pea (*Clitoria ternatea*) seed and petal extracts decreased HEp-2 carcinoma cell viability. International Journal of Food Science & Technology, 51(8), 1860–1868.
- Shivaprakash, P., Balaji, K. S., Chandrashekara, K. T., Rangappa, K. S., & Jayarama, S. (2015). Induction of apoptosis in MCF-7 cells by methanolic extract of *Clitoria ternatea* L. International Journal of Applied Biology and Pharmaceutical Technology, 6, 80–86.
- Tate, J. G., Bamford, S., Jubb, H. C., Sondka, Z., Beare, D. M., Bindal, N., et al. (2019). COSMIC: the Catalogue Of Somatic Mutations In Cancer. Nucleic Acids Research, 47(D1), D941–D947.
- Trott, O., & Olson, A. J. (2010). AutoDock Vina: improving the speed and accuracy of docking with a new scoring function, efficient optimization, and multithreading. Journal of Computational Chemistry, 31, 455–461.
- Usui, T., Shizuuchi, S., Watanabe, H., & Hayase, F. (2004). Cytotoxicity and oxidative stress induced by the glyceraldehyde-related Maillard reaction products for HL-60 cells. Bioscience, Biotechnology, and Biochemistry, 68(2), 333–340.
- Zhang, S., Xiao, K. Z., Jin, J., Zhang, Y., & Zhou, W. (2013). Chemosensitizing activities of cyclotides from *Clitoria ternatea* in paclitaxel-resistant lung cancer cells. Oncology Letters, 5(2), 641–644.